

University of Nebraska - Lincoln

DigitalCommons@University of Nebraska - Lincoln

---

David Sellmyer Publications

Research Papers in Physics and Astronomy

---

11-1-2002

## Curie temperature of FePt:B<sub>2</sub>O<sub>3</sub> nanocomposite films

H. Zeng

*University of Nebraska - Lincoln*

Renat F. Sabirianov

*Stanford University, rsabirianov@mail.unomaha.edu*

O. Mryasov

*Seagate Research, Pittsburgh, Pennsylvania*

M.L. Yan

*University of Nebraska - Lincoln*

K. Cho

*Department of Materials Science and Engineering, Stanford University, Stanford, California*

*See next page for additional authors*

Follow this and additional works at: <https://digitalcommons.unl.edu/physicsellmyer>

 Part of the [Physics Commons](#)

---

Zeng, H.; Sabirianov, Renat F.; Mryasov, O.; Yan, M.L.; Cho, K.; and Sellmyer, David J., "Curie temperature of FePt:B<sub>2</sub>O<sub>3</sub> nanocomposite films" (2002). *David Sellmyer Publications*. 39.

<https://digitalcommons.unl.edu/physicsellmyer/39>

This Article is brought to you for free and open access by the Research Papers in Physics and Astronomy at DigitalCommons@University of Nebraska - Lincoln. It has been accepted for inclusion in David Sellmyer Publications by an authorized administrator of DigitalCommons@University of Nebraska - Lincoln.

---

**Authors**

H. Zeng, Renat F. Sabirianov, O. Mryasov, M.L. Yan, K. Cho, and David J. Sellmyer

## Curie temperature of FePt:B<sub>2</sub>O<sub>3</sub> nanocomposite films

H. Zeng,<sup>1,\*</sup> R. Sabirianov,<sup>2</sup> O. Mryasov,<sup>3</sup> M. L. Yan,<sup>1</sup> K. Cho,<sup>2</sup> and D. J. Sellmyer<sup>1</sup>

<sup>1</sup>Center for Materials Research and Analysis and Department of Physics and Astronomy, University of Nebraska, Lincoln, Nebraska 68588

<sup>2</sup>Department of Materials Science and Engineering, Stanford University, Stanford, California 94305

<sup>3</sup>Seagate Research, 1251 Waterfront Place, Pittsburgh, Pennsylvania 15222

(Received 13 May 2002; revised manuscript received 3 September 2002; published 22 November 2002)

We report results on experimental and theoretical studies of structural and magnetic properties of FePt:B<sub>2</sub>O<sub>3</sub> nanocomposite films. It was found for films prepared by magnetron sputtering with subsequent annealing that lattice parameters  $a$  and  $c$  of fct FePt change with significantly different rates with increase of the B<sub>2</sub>O<sub>3</sub> fraction. As a consequence, fundamental magnetic properties change markedly, with the Curie temperature decreasing by 36% for 25% FePt volume fraction compared with the bulk value. Using an *ab initio* parametrization of magnetic interactions, we propose statistical model of thermal fluctuations in fct FePt, which explains these observations. Our modeling results demonstrate that the observed phenomena originate in the variation of the exchange interaction parameters with the changes in the  $c/a$  ratio. We find that the main factor of this variation is the increase of the difference between the in-plane and interplane exchange interactions as  $c/a$  decreases from its bulk value due to stress exerted by the B<sub>2</sub>O<sub>3</sub> matrix.

DOI: 10.1103/PhysRevB.66.184425

PACS number(s): 75.50.Ss, 75.50.Kj, 75.50.Cc

### INTRODUCTION

$L1_0$ -ordered FePt and CoPt alloys exhibit strong magnetocrystalline anisotropy ( $K_u > 3 \times 10^7$  erg/cm<sup>3</sup>), and have potential applications as permanent magnets.<sup>1</sup> Recently, dense arrays of FePt nanoparticles were produced by self-assembly and proposed as magnetic storage media materials with an areal density greater than 1 terabit/in<sup>2</sup>.<sup>2</sup> An alternative approach of achieving high areal density of magnetic grains is the employing of nanocomposite films with  $L1_0$  structured CoPt and FePt nanoparticles embedded in a nonmagnetic matrix such as C, SiO<sub>2</sub>, B<sub>2</sub>O<sub>3</sub>, and BN.<sup>3-6</sup> It is expected that these films possess a high anisotropy of CoPt or FePt grains; meanwhile, nanoparticles are separated by matrix materials to reduce the intergrain exchange coupling. To date, few studies were devoted to understanding the fundamental properties such as the magnetization, magnetocrystalline anisotropy, and exchange interactions of such films, with the addition of the matrix materials. It is a common practice to assume that the magnetic properties of these nanocomposite films can be represented by intrinsic properties of their magnetic components in their bulk form.<sup>7</sup> However, it is well known that intrinsic magnetic properties might be very sensitive to the local atomic environment. By alloying with other elements, or by embedding nanocrystallites in a matrix, it can be expected that the electronic structure of the magnetic grains be modified so that the intrinsic properties change accordingly. This is especially true for Fe-based alloys that show variety of unusual pressure and temperature properties.

In this paper, we present a systematic analysis of the structure and magnetic properties of FePt:B<sub>2</sub>O<sub>3</sub> nanocomposite films with varying FePt volume fraction, in order to understand the change of fundamental properties with the addition of a B<sub>2</sub>O<sub>3</sub> matrix. In these films, FePt near a 50/50 composition possesses hard magnetic properties, while B<sub>2</sub>O<sub>3</sub> is an amorphous insulator. We show that structural proper-

ties, such as the lattice parameters are modified by the addition of B<sub>2</sub>O<sub>3</sub>. Furthermore, the measured Curie temperature ( $T_c$ ) for these films reduces strongly with a decrease of FePt concentration in the composite. To understand this somewhat unexpected observation we perform an analysis of elastic, magnetic and electronic properties of FePt. We employ statistical modeling and *ab initio* calculations to address the fundamental question of the nature of exchange interactions and anisotropy in this system.

### I. EXPERIMENTAL RESULTS

(FePt) <sub>$x$</sub> :(B<sub>2</sub>O<sub>3</sub>)<sub>1- $x$</sub>  nanocomposite films were prepared by magnetron sputtering Fe/Pt:B<sub>2</sub>O<sub>3</sub> multilayers onto glass substrates, followed by a subsequent annealing at 825 K for 24 h. The FePt volume fraction was varied from 100%, or a pure FePt film, to 25%, where FePt grains are mostly isolated by amorphous B<sub>2</sub>O<sub>3</sub>. The total film thicknesses ranged from 100 to 400 nm to keep the FePt thickness fixed at 100 nm. The structural properties were characterized by x-ray diffraction (XRD) and transmission electron microscopy (TEM). Magnetization from room temperature to 800 K was measured by a vibrating-sample magnetometer, where  $T_c$  was determined by the inflection point of the  $M(T)$  curve.

Upon annealing, the multilayer configuration of the films is broken, and nanocomposite films with FePt nanocrystallites embedded in the amorphous B<sub>2</sub>O<sub>3</sub> matrix are formed. At the same time, FePt forms an ordered face-centered-tetragonal crystal structure.<sup>5</sup> Figure 1 shows representative XRD patterns of FePt:B<sub>2</sub>O<sub>3</sub> samples with FePt volume fractions from 100% to 25%. One interesting feature is that the (111) peak position only changes slightly with the FePt volume fraction; however, (001) and (002) peaks shift significantly to large angles as the FePt volume fraction decreases. This suggests that as the nonmagnetic matrix concentration increases, the lattice of FePt grains becomes more and more distorted. For fct FePt, the lattice constant  $c$  is slightly

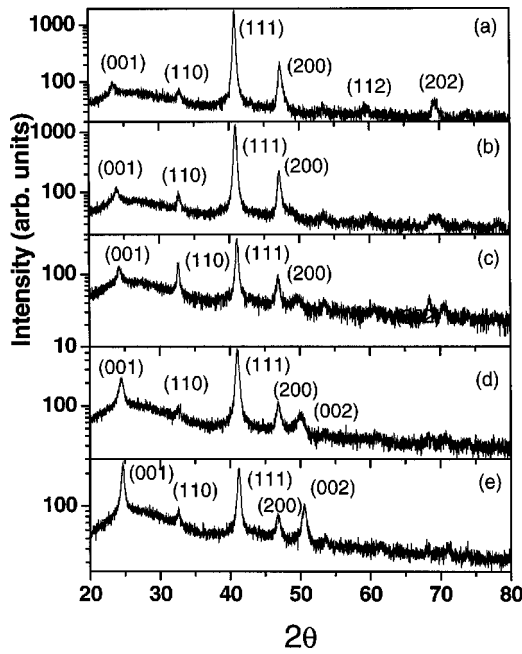


FIG. 1. Representative XRD patterns of  $(\text{FePt})_x:(\text{B}_2\text{O}_3)_{1-x}$ , with (a)  $x = 100$ , (b)  $x = 80$ , (c)  $x = 60$ , (d)  $x = 40$ , and (e)  $x = 25$ .

smaller than  $a$ . The shift of  $(00n)$  peaks to higher angles indicates the decrease of the  $c$  spacing. The calculated lattice constants  $c$  and  $a$  as well as the  $c/a$  ratio as a functions of the FePt volume fraction are plotted in Fig. 2. As can be seen from Fig. 2, for a pure FePt film,  $a$ ,  $c$ , and  $c/a$  are 3.85 Å, 3.74 Å and  $c/a$  0.97, respectively, which are fairly close to the bulk values.<sup>8</sup> It can be seen that as the FePt volume fraction decreases from 100% to 25%,  $a$  only increases slightly from 3.85 to 3.88 Å. However,  $c$  decreases considerably from 3.74 to 3.61 Å, which is a 3.5% change. As a consequence, the  $c/a$  ratio decreases from 0.97 for pure FePt to 0.93 for the film contains 25% FePt. This change is pre-

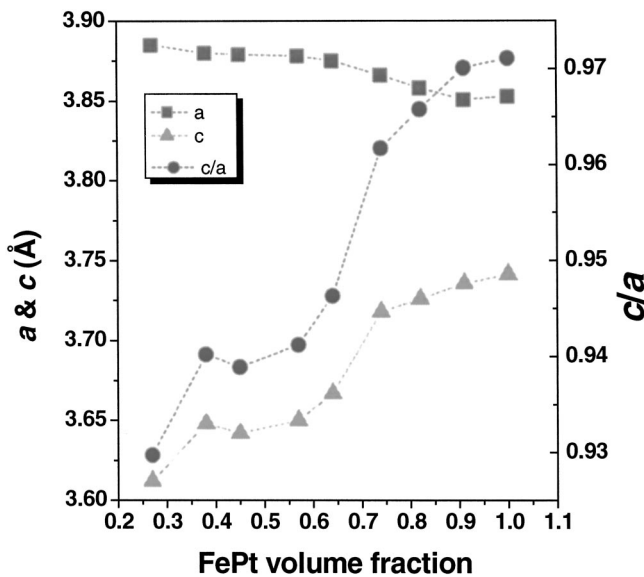


FIG. 2. Lattice parameters  $a$ ,  $c$  and  $c/a$  ratio as a function of the FePt volume fraction.

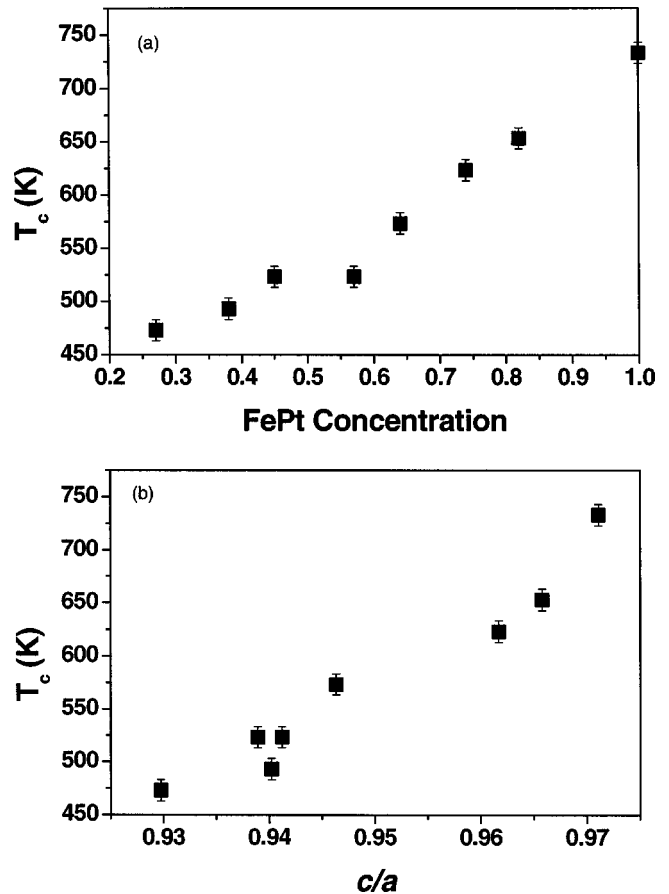


FIG. 3. The Curie temperature  $T_c$  as a function of (a) the FePt volume fraction and (b) the  $c/a$  ratio.

sumably due to the strain exerted by the matrix on the FePt lattice. As shown below, the change in the  $c/a$  ratio has a strong influence on the Curie temperature  $T_c$  of the films.

For the films studied, the average grain sizes as estimated from Scherrer's formula range from 25 nm for pure FePt to 15 nm for a 25% volume fraction of FePt. TEM images reveal that for a high FePt volume fraction, most FePt grains are interconnected, while for a FePt volume fraction less than 30%, FePt grains are well isolated. A statistical analysis shows that the mean grain size for the sample with isolated grains is very close to XRD results. There is a substantial grain size distribution, with  $\delta d/d \sim 30\%$ , where  $d$  is the grain diameter. However, the number of grains with diameter less than 10 nm only accounts for a small portion.

Shown in Fig. 3(a) is  $T_c$  as a function of the FePt volume fraction.  $T_c$  for a pure FePt film is 733 K, which is close to the bulk value of 750 K. However, as the FePt volume fraction changes from 100% to 25%,  $T_c$  decreases almost linearly to 470 K. The total reduction is 263 K, about 36% of the bulk value. This reduction correlates with the change in the  $c/a$  ratio with variation of the FePt volume fraction. Figure 3(b) shows  $T_c$  as a function of the  $c/a$  ratio.

The origin of such a behavior may be associated with two groups of factors. First there is the partial ordering of FePt grains with the increase of the  $\text{B}_2\text{O}_3$  concentration or the diffusion of impurities such as B or O in FePt. The second

group of factors includes phenomena intrinsic to the system such as (i) superparamagnetism of smaller grains,<sup>9</sup> (ii) surface effects due to the change of coordination at the interface between FePt and B<sub>2</sub>O<sub>3</sub>, and (iii) a reduction of the exchange interaction parameters with changes of the lattice parameters.

Concerning partial ordering due to insufficient thermal treatment that may affect  $T_c$ , we carefully examined the effect of annealing. Our pure FePt film shows only a slight decrease in  $T_c$  as compared to bulk, suggesting that the disorder is small. The addition of B<sub>2</sub>O<sub>3</sub>, however, significantly hinders the phase formation. In order to achieve nearly perfect ordering, 24-h annealing is performed on all samples. Prolonged annealing leads to no significant change in  $T_c$ . The (001) and (002) peak intensity ratios of XRD for 25% FePt are similar to that of bulk fct FePt, suggesting that the FePt crystallites are well ordered even for a low FePt volume fraction.

Finite-size effects of nanocomposite films may contribute to the variation of  $T_c$  as well.<sup>10</sup> However, since all samples have average grain sizes greater than 15 nm, and the number of grains with diameter smaller than 10 nm is negligible, and since the behavior of 15-nm grains already resemble that of bulk, it can be anticipated that finite-size contribution is insignificant. It is established for clusters of different materials that only one surface layer (or two) are substantially affected by surface disorder. Models of magnetically dead layer describe successfully variation of magnetization in number of systems. The grain sizes are large in our experiment. If we assume dead layer to be 2 Å thick, less than 9% of atoms for 15 nm and less than 5.5% for 25 nm are in the surface layer. Thus the direct effect will be small. Nevertheless, because interface area between FePt and B<sub>2</sub>O<sub>3</sub> phases increases from 0 to almost 100% with a decrease in the FePt concentration, we expect this dead layer effect to be of the order of 5–10%.

The saturation magnetization of the films is a linear function of the FePt volume fraction, suggesting dilution effects, and the Fe local moment is unchanged. We do not expect a significant diffusion between FePt and B<sub>2</sub>O<sub>3</sub> phases.

## II. THEORETICAL RESULTS AND DISCUSSIONS

To understand the origin of the observed trend in the magnetic properties of FePt:B<sub>2</sub>O<sub>3</sub> nanocomposite films, we perform two sets of *ab initio* calculations: (i) calculations of total energy to model the effect of external stress exerted by the composite matrix, and (ii) calculations of the exchange interaction parameters as a function of the FePt unit cell volume and the  $c/a$  ratio. Finally, we perform Monte Carlo simulations for the tetragonal lattice with anisotropy of exchange interactions. We obtain the Curie temperature change as a function of interlayer exchange and consequently as a function of the  $c/a$  ratio.

We employ the linear-muffin-tin-orbital (LMTO) method in the atomic-sphere approximation (ASA) for most of the electronic structure calculations.<sup>11</sup> This method approximates the shape of the potential with a muffin-tin form. The full-potential version of the LMTO (FLMTO) method has lifted this approximation,<sup>12</sup> and is used for total energy calcula-

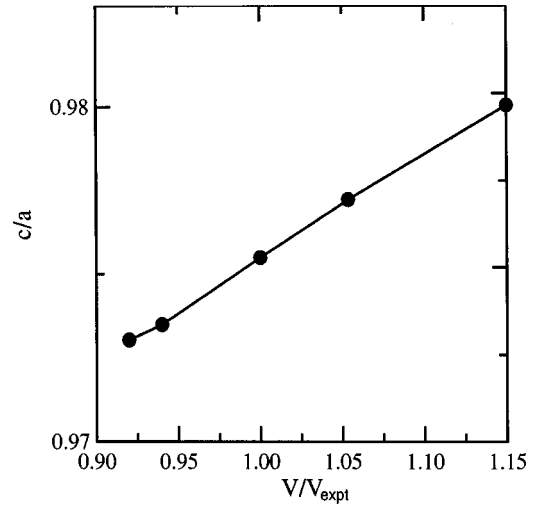


FIG. 4. Calculated equilibrium  $c/a$  ratio as a function of the volume normalized by the experimental value of pure FePt ( $V_{\text{expt}}$ ).

tions. The Green's-function method is used to calculate pair exchange parameters. Green's functions are calculated from the self-consistent solution of the LMTO-ASA method.<sup>13,14</sup> The exchange interaction calculations in FePt are quite sensitive to the details of the electronic structure. Because of this, the local-spin-density approximation+Hubbard  $U$  approximation (LSDA+ $U$ ) calculations in scope of the LMTO-ASA method have been performed to study the effect of correlations on the interlayer exchange coupling.<sup>15</sup> The effect of spin-orbit coupling is studied as well. The above methods are widely used in the solid-state physics and more detailed information can be found in the above references.

### A. Elastic properties calculation

Using the FLMTO method we calculated the equilibrium  $c/a$  variation as a function of the volume reduced to the experimental value of pure FePt. As can be seen from Fig. 4, the  $c/a$  ratio decreases with the decrease of the volume (or increase in pressure). This result is consistent with experimental observations and shows that the LSDA model describes qualitatively the difference in the response of  $c/a$  and  $a$  parameters on the external stress. Although calculated differences in  $a$  and  $c/a$  variations are somewhat underestimated in comparison with experimental results. Besides the LSDA problem, the reason for this may be nonuniform stress from the matrix or some interdiffusion of boron or oxygen.

### B. Exchange interactions and magnetic properties

Determining exchange coupling in the system requires a mapping of the energy change on the rotation of the local magnetic moment. The response can be found in two ways: (1) analytically for an infinitesimal angle rotation, and (2) numerically for a finite angle rotation. We will use and compare both approaches.

To determine the parameters of magnetic interactions and correspondingly the energetic of thermal fluctuations in FePt, we use infinitesimal angle rotations of magnetic moments around the ferromagnetic ground state. In the case of small

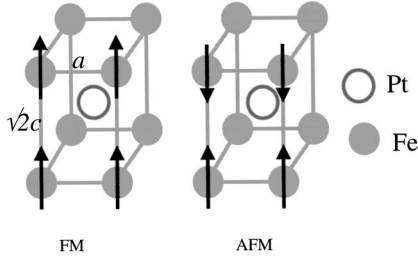


FIG. 5. Schematic illustration of a FePt unit cell with (a) ferromagnetic (FM) and (b) antiferromagnetic (AFM) configurations of magnetic moments between neighboring Fe planes.

deviations from the ground state, the problem can be solved within perturbation theory. The use of the LSDA extension of the local force theorem and multiple-scattering formulation of the perturbation theory allows the derivation of a closed-form expression for exchange interaction parameters.<sup>13</sup> This approach assumes that the exchange interaction energy can be accurately mapped into the Heisenberg form

$$H = - \sum_{ij} J_{ij} \vec{S}_i \cdot \vec{S}_j, \quad (1)$$

with pair effective interaction parameters  $J_{ij}$  and  $S_i$  being unit vectors in the direction of the local moment. Since this method also assumes that the deviation from the ground state is such that perturbation theory is valid, we will call this approach the infinitesimal angle approach. Within second-order perturbation theory the coupling parameters are given by the expression

$$\Delta E = J_{ij} \theta^2 = \left\{ \frac{1}{\pi} \text{Im} \int_{-\infty}^{E_F} dE \Delta t_i^{-1} T_{0ij}^\dagger \Delta t_j^{-1} T_{0ji}^\dagger \right\} \theta^2 \quad (2)$$

where  $J_{ij}$  are exchange coupling parameters,  $T_{0ij}^{\uparrow,\downarrow}$  is the scattering path operator in site representation,  $\Delta t_i^{-1} = t_{i\uparrow}^{-1} - t_{i\downarrow}^{-1}$  is the difference of inverse single-site scattering matrices, and  $\theta$  is the rotation angle.  $T_{0ij}^{\uparrow,\downarrow}$  has a simple scaling relationship with Green's function and we will refer to the above approach as Green's-function method.  $t_{i\uparrow}^{-1}$  is a potential function of the LMTO method. The on-site (total) exchange parameter  $J_0 = \sum_j J_{0j}$  can be calculated analytically as well.<sup>13</sup> The sum in the equation is over all the neighbors around site 0. More details can be found in Ref. 14.

FePt has a layered structure with alternating Fe and Pt planes, as shown in Fig. 5. It can be also viewed as a tetragonally distorted fcc lattice. From LMTO-ASA calculations (without spin-orbit coupling), Fe has a local magnetic moment of  $2.85\mu_B$  and Pt has an induced atomic moment of  $0.4\mu_B$ . The calculated exchange parameters show a strong coupling in the Fe planes and weaker coupling between planes. There is, furthermore, a comparable contribution from the coupling between the Fe and Pt planes. This indicates that, though that magnetic moment induced on Pt atoms is relatively small, its role in the formation of effective exchange fields cannot be ignored. On the other hand, since the Pt moment is induced and essentially very delocalized, the use of infinitesimal angle mapping to the Heisenberg

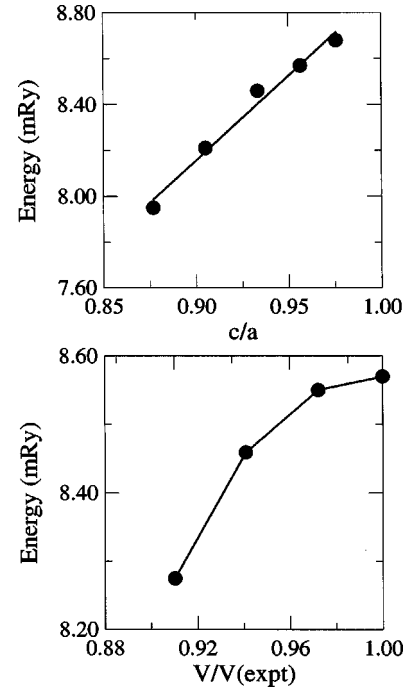


FIG. 6. The calculated on-site (total) exchange parameters  $J_0$  as a function of (a) the  $c/a$  ratio and (b) the unit cell volume.

model [Eq. (2)] may introduce a significant error in estimations of the critical temperature. To interrogate our model further we performed calculations of exchange interaction energy between Fe planes using a finite-angle rotation. We use a finite-angle rotation of the magnetization between neighboring planes of Fe to calculate the coupling<sup>16</sup> between the iron planes to elucidate possible deviations from behaviors that can be derived from Eqs. (1) and (2). We calculated the total energy difference between ferromagnetically and antiferromagnetically aligned planes. In the antiferromagnetic (AFM) configuration Pt has a zero moment while the Fe moment remains essentially unchanged from the value of the ferromagnetic (FM) configuration. This result indicates that the infinitesimal angle parametrization of the exchange energy might not be sufficiently accurate in describing exchange interactions between Fe planes due to mediating effects of the Pt moment which appears to be very sensitive to magnetic configurations.

In Fig. 6 we present the calculated on-site exchange parameter (defined for the Fe site) as a function of the  $c/a$  ratio and volume. For an interpretation of our experimental results it is important to notice that combined effects of  $c/a$  and volume variations may account for about a 0.2-mRy reduction of the on-site exchange parameter. However, considering the contribution of different pairs to the total exchange coupling parameter, we notice that in-plane iron has a very strong coupling that does not change much with  $c/a$  or volume variations, while exchange between planes is strongly affected by these structural changes.

In Fig. 7 we present calculated differences between magnetic moments of FM and AFM aligned Fe layers. One can see strong reduction of the interplane exchange coupling with the reduction of the  $c/a$  ratio. Because there is strong

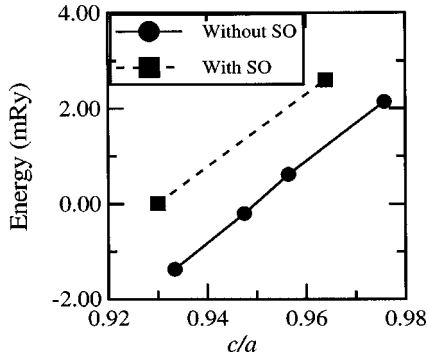


FIG. 7. The energy difference between AFM and FM configurations (the positive sign corresponds to the FM coupling) as a function of the  $c/a$  ratio. The inclusion of SO coupling shifts the energy difference toward FM order.

in-plane coupling between Fe sites, the system can be considered as layered. The planes have strongly ordered local moments and the coupling between the moments of the planes is weaker. Overall, the LSDA-based results are consistent with the  $T_c$  reduction observed experimentally. However, finite-angle calculations of Fe-Fe interlayer exchange overestimates the dependence on the  $c/a$  ratio, and result in erroneous negative values for  $c/a=0.945$ . In order to make sure that the ASA does not produce a substantial error we have checked the results using projector augmented wave method adopted at VASP (Ref. 17) for  $c/a=0.93$ , and found that the AFM order is indeed more stable.

To investigate whether this negative exchange energy is coming from the LSDA approximation, we performed LSDA+ $U$  calculations, which allow us to take into account on-site Coulomb correlation in more consistent ways than the LSDA.<sup>15</sup> We used  $U=1.52$  eV on Fe and  $U=0.54$  eV on Pt, the values of Coulomb correlation parameters which allows reproducing within the LSDA+ $U$  model experimental results for both magnetocrystalline anisotropy, atom-resolved total magnetic moments, and to some degree atom-resolved orbital moments.<sup>18</sup> We find, however, that the interplane exchange energy has not been changed significantly due to correlations. Thus we conclude that the overestimation of the trend should be due to different sources.

We found that if spin-orbit (SO) coupling is included in the calculation, the results change significantly, indicating the importance of this type of interaction. We have calculated  $E(\text{AFM})-E(\text{FM})$  differences both including an  $f$  orbital in the basis set and with SO interaction included self-consistently. Calculations were performed using the Barth-Hedin<sup>19</sup> exchange-correlation potential and tetrahedron integration over an irreducible Brillouin zone wedge with  $31 \times 31 \times 15$   $k$ -point sampling. Results clearly indicate that the role of SO coupling is increasing the stability of FM order by about 1 mRy (Fig. 7). For the FM configuration Pt has a spin moment of 0.4, while it has no moment in the AFM configuration. As a result SO coupling makes a large contribution to the exchange interaction energy and correspondingly to the ordering temperature.

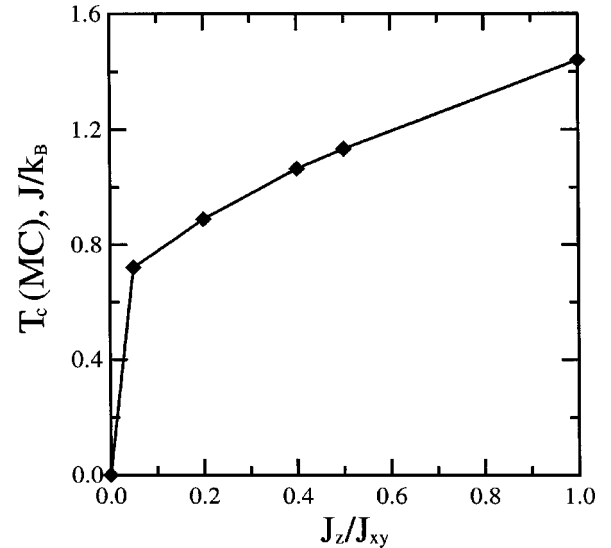


FIG. 8. Curie temperature for a simple cubic lattice with nearest-neighbor interactions as a function of the ratio between interplane ( $J_z$ ) and in-plane ( $J_{xy}$ ) exchange parameters.

### C. Monte Carlo simulations

As we stated above, the main effect of the  $c/a$  change with increase of B<sub>2</sub>O<sub>3</sub> concentration is a reduction of the interplane exchange coupling. The effect of this reduction on the Curie temperature is not *a priori* clear. In order to clarify this point we have performed Monte Carlo (MC) simulations of a simple cubic structure with nearest-neighbor interactions, where we fix each pair in-plane exchange coupling parameter at 1 and vary the interplane coupling from 1 to 0. Figure 8 shows  $T_c$  as a function of the ratio of interplane to inplane exchange,  $R=J_{ii'}/J_{ij}$ . We can see that  $T_c$  decreases from 1.44( $J/k_B$ ) ( $k_B$  is the Boltzmann constant) for  $R=1$  to 0.7( $J/k_B$ ) for  $R=0.05$ . Interestingly, we have noticed that the  $T_c$  reduction is initially proportional to the decrease of the on-site (total) exchange parameter  $J_0$ , up until  $R \sim 0.5$ , then accelerates with further decreasing  $R$ . This means that mean-field theory is not able to explain the variation of  $T_c$  in systems with a directional anisotropy of exchange interactions, and is not applicable directly to the layered systems such as FePt.

The Green-function calculations [Eq. (2)] show that in-plane exchange is about 8 mRy. It is very strong for the first two shells of neighbors and has long-range oscillations. The interplane exchange calculated by finite-angle rotation changes from 2 mRy to very small numbers with a reduction of the  $c/a$  ratio. In terms of the model used in MC simulations, it corresponds to changes in  $R$  from 0.25 to quite small values. One then can expect a strong reduction of Curie temperatures for the  $c/a$  ratios observed experimentally. We estimate that Curie temperature falls by about 30% (it would be only 10% in mean-field theory) if the  $R$  ratio drops from 0.25 to 0.05 by means of an interplane exchange parameter reduction. This roughly corresponds to the experimental results. Thus the reduction of the interplane exchange parameter alone is satisfactory in explaining the strong decrease in  $T_c$ .

Although the Curie temperature variation is explained well by this mechanism, additional effects may play roles as well. Some reduction may be attributed to substitutional disorder in FePt, which is quite small, as observed. Some reduction may be explained at least in part by the chemical disorder due to the B or O interdiffusion into FePt in small amounts. Finally the surface atoms may have reduced exchange coupling and random anisotropy may cause some reduction in  $T_c$ .

### CONCLUSIONS

In summary, we have studied the magnetic properties of FePt grains embedded into a matrix of boron oxide as a function of the FePt content. We find that the  $B_2O_3$  matrix produces strong stress on the FePt clusters, reducing the  $c/a$  ratio and the unit volume of the FePt phase. The Curie temperature decreases with decreasing FePt content from 750 K for pure FePt to 470 K for 25% FePt ( $c/a$  decreases from 0.97 to 0.93). In order to interpret these experimental results we performed two sets of *ab initio* calculations. We find that the difference in the variation of  $c/a$  and  $a$  structural param-

eters can be explained within LSDA total-energy calculations. We find that the calculated variation of the exchange parameters may account for the reduction of the Curie temperature. The in-plane exchange coupling does not change much with the  $c/a$  ratio or volume reduction, while interplane exchange coupling parameter decreases significantly with  $c/a$  reduction. Monte Carlo calculations of the critical temperature using exchange interactions, calculated from first principles, show a reduction of  $T_c$  by about 30%, in agreement with experiments. Thus we conclude that the main contribution to the observed changes in the magnetic behavior with the decrease of FePt volume fraction originates from the renormalization of exchange interaction parameters. Particularly, due to the increased difference between the inter- and intra-layer interaction parameters with the structural change of FePt nanocrystallites.

### ACKNOWLEDGMENTS

The authors thank S. Jaswal for fruitful discussions and X. Z. Li for TEM observations. This research was supported by the NSF, NRI, IBM, and CMRA.

\*Present address: IBM T.J. Watson Research Center, Yorktown Heights, New York, 10598. Email address: haozeng@us.ibm.com

<sup>1</sup>Y. Tanaka, N. Kimura, K. Hono, K. Yasuda, and T. Sakurai, *J. Magn. Magn. Mater.* **170**, 289 (1997).

<sup>2</sup>S. Sun, C. B. Murray, D. Weller, L. Folks, and A. Moser, *Science* **287**, 1989 (2000).

<sup>3</sup>M. Yu, Y. Liu, and D. J. Sellmyer, *Appl. Phys. Lett.* **75**, 3992 (1999).

<sup>4</sup>C. P. Luo and D. J. Sellmyer, *Appl. Phys. Lett.* **75**, 3162 (1999).

<sup>5</sup>C. P. Luo, S. H. Liou, L. Gao, Y. Liu, and D. J. Sellmyer, *Appl. Phys. Lett.* **77**, 2225 (2000).

<sup>6</sup>J. A. Christodoulides, Y. Huang, Y. Zhang, G. C. Hadjipanayis, I. Panagiotopoulos, and D. Niarchos, *J. Appl. Phys.* **87**, 6938 (2000).

<sup>7</sup>S. Stavroyiannis, I. Panagiotopoulos, D. Niarchos, J. A. Christodoulides, Y. Zhang, and G. C. Hadjipanayis, *Appl. Phys. Lett.* **73**, 3453 (1998).

<sup>8</sup>JCPD card, 43-1359.

<sup>9</sup>R. W. Chantrell, D. Weller, T. J. Klemmer, S. Sun, and E. E. Fullerton, *J. Appl. Phys.* **91**, 6866 (2002).

<sup>10</sup>A. Gavrin and C. L. Chien, *J. Appl. Phys.* **73**, 6949 (1993).

<sup>11</sup>O. K. Andersen, *Phys. Rev. B* **8**, 3060 (1975).

<sup>12</sup>M. Methfessel and M. van Schilfhaarde, *Phys. Rev. B* **48**, 4937 (1993).

<sup>13</sup>A. Liechtenstein, V. Antropov, M. Katsnelson, and V. Gubanov, *J. Magn. Magn. Mater.* **67**, 65 (1987).

<sup>14</sup>R. F. Sabiryanov, S. K. Bose, and O. N. Mryasov, *Phys. Rev. B* **51**, 8958 (1995).

<sup>15</sup>O. N. Mryasov, R. F. Sabiryanov, A. J. Freeman, and S. S. Jaswal, *Phys. Rev. B* **56**, 7255 (1997).

<sup>16</sup>I. V. Solovyev, P. H. Dederichs, and V. I. Anisimov, *Phys. Rev. B* **50**, 16 861 (1994).

<sup>17</sup>G. Kresse and D. Joubert, *Phys. Rev. B* **59**, 1758 (1999).

<sup>18</sup>A. Schick and O. Mryasov (unpublished).

<sup>19</sup>U. von Barth and L. Hedin, *J. Phys. C* **5**, 1629 (1972).